EDITOR IN CHIEF

Rudy J. M. Konings
European Commission, Joint Research Centre,
Institute for Transuranium Elements, Karlsruhe, Germany

SECTION EDITORS

Todd R. Allen
Department of Engineering Physics, University of Wisconsin, Madison, WI, USA

Roger E. Stoller
Materials Science and Technology Division, Oak Ridge National Laboratory, Oak Ridge, TN, USA

Shinsuke Yamanaka
Division of Sustainable Energy and Environmental Engineering, Graduate School of Engineering, Osaka University, Osaka, Japan

Elsevier
Radarweg 29, PO Box 211, 1000 AE Amsterdam, The Netherlands
The Boulevard, Langford Lane, Kidlington, Oxford OX5 1GB, UK
225 Wyman Street, Waltham, MA 02451, USA

British Library Cataloguing in Publication Data
A catalogue record for this book is available from the British Library

Library of Congress Catalog Number: 2011929343

ISBN (print): 978-0-08-056027-4

For information on all Elsevier publications
visit our website at books.elsevier.com

Cover image courtesy of Professor David Sedmidubský, The Institute of Chemical Technology, Prague

Printed and bound in Spain

12 13 14 15 16 10 9 8 7 6 5 4 3 2 1

Editorial: Gemma Mattingley
Production: Nicky Carter

EDITORS BIOGRAPHIES

Rudy Konings is currently head of the Materials Research Unit in the Institute for Transuranium Elements (ITU) of the Joint Research Centre of the European Commission. His research interests are nuclear reactor fuels and actinide materials, with particular emphasis on high temperature chemistry and thermodynamics. Before joining ITU, he worked on nuclear fuel-related issues at ECN (the Energy Research Centre of the Netherlands) and NRG (Nuclear Research and Consultancy Group) in the Netherlands. Rudy is editor of *Journal of Nuclear Materials* and is professor at the Delft University of Technology (Netherlands), where he holds the chair of 'Chemistry of the nuclear fuel cycle.'

Roger Stoller is currently a Distinguished Research Staff Member in the Materials Science and Technology Division of the Oak Ridge National Laboratory and serves as the ORNL Program Manager for Fusion Reactor Materials for ORNL. He joined ORNL in 1984 and is actively involved in research on the effects of radiation on structural materials and fuels for nuclear energy systems. His primary expertise is in the area of computational modeling and simulation. He has authored or coauthored more than 100 publications and reports on the effects of radiation on materials, as well as edited the proceedings of several international conferences.

Todd Allen is an Associate Professor in the Department of Engineering Physics at the University of Wisconsin – Madison since 2003. Todd's research expertise is in the area of materials-related issues in nuclear reactors, specifically radiation damage and corrosion. He is also the Scientific Director for the Advanced Test Reactor National Scientific User Facility as well as the Director for the Center for Material Science of Nuclear Fuel at the Idaho National Laboratory, positions he holds in conjunction with his faculty position at the University of Wisconsin.

Shinsuke Yamanaka is a professor in Division of Sustainable Energy and Environmental Engineering, Graduate School of Engineering, Osaka University since 1998. He has studied the thermophysics and thermochemistry of nuclear fuel and materials. His research for the hydrogen behavior in LWR fuel cladding is notable among his achievements and he received the Young Scientist Awards (1980) and the Best Paper Awards (2004) from Japan Atomic Energy Society. Shinsuke is the program officer of Japan Science and Technology Agency since 2005 and the visiting professor of Fukui University since 2009, and he is also the associate dean of Graduate School of Engineering, Osaka University since 2011.

PREFACE

There are essentially three primary energy sources for the billions of people living on the earth's surface: the sun, radioactivity, and gravitation. The sun, an enormous nuclear fusion reactor, has transmitted energy to the earth for billions of years, sustaining photosynthesis, which in turn produces wood and other combustible resources (biomass), and the fossil fuels like coal, oil, and natural gas. The sun also provides the energy that steers the climate, the atmospheric circulations, and thus 'fuelling' wind mills, and it is at the origin of photovoltaic processes used to produce electricity. Radioactive decay of primarily uranium and thorium heats the earth underneath us and is the origin of geothermal energy. Hot springs have been used as a source of energy from the early days of humanity, although it took until the twentieth century for the potential of radioactivity by fission to be discovered. Gravitation, a non-nuclear source, has been long used to generate energy, primarily in hydropower and tidal power applications.

Although nuclear processes are thus omnipresent, nuclear technology is relatively young. But from the moment scientists unraveled the secrets of the atom and its nucleus during the twentieth century, aided by developments in quantum mechanics, and obtained a fundamental understanding of nuclear fission and fusion, humanity has considered these nuclear processes as sources of almost unlimited (peaceful) energy. The first fission reactor was designed and constructed by Enrico Fermi in 1942 in Chicago, the CP1, based on the fission of uranium by neutron capture. After World War II, a rapid exploration of fission technology took place in the United States and the Union of Soviet Socialist Republics, and after the Atoms for Peace speech by Eisenhower at the United Nations Congress in 1954, also in Europe and Japan. A variety of nuclear fission reactors were explored for electricity generation and with them the fuel cycle. Moreover, the possibility of controlled fusion reactions has gained interest as a technology for producing energy from one of the most abundant elements on earth, hydrogen.

The environment to which materials in nuclear reactors are exposed is one of extremes with respect to temperature and radiation. Fuel pins for nuclear reactors operate at temperatures above 1000 °C in the center of the pellets, in fast reactor oxide fuels even above 2000 °C, whereas the effects of the radiation (neutrons, alpha particles, recoil atoms, fission fragments) continuously damage the material. The cladding of the fuel and the structural and functional materials in the fission reactor core also operate in a strong radiation field, often in a dynamic corrosive environment of the coolant at elevated temperatures. Materials in fusion reactors are exposed to the fusion plasma and the highly energetic particles escaping from it. Furthermore, in this technology, the reactor core structures operate at high temperatures. Materials science for nuclear systems has, therefore, been strongly focussed on the development of radiation tolerant materials that can operate in a wide range of temperatures and in different chemical environments such as aqueous solutions, liquid metals, molten salts, or gases.

The lifetime of the plant components is critical in many respects and thus strongly affects the safety as well as the economics of the technologies. With the need for efficiency and competitiveness in modern society, there is a strong incentive to improve reactor components or to deploy advanced materials that are continuously developed for improved performance. There are many examples of excellent achievements in this respect. For example, with the increase of the burnup of the fuel for fission reactors, motivated by improved economics and a more efficient use of resources, the Zircaloy cladding (a Zr–Sn alloy) of the fuel pins showed increased susceptibility to coolant corrosion, but within a relatively short period, a different zirconium-based alloy was developed, tested, qualified, and employed, which allowed reliable operation in the high burnup range.

Nuclear technologies also produce waste. It is the moral obligation of the generations consuming the energy to implement an acceptable waste treatment and disposal strategy. The inherent complication of radioactivity, the decay that can span hundreds of thousands of years, amplifies the importance of extreme time periods in the issue of corrosion and radiation stability. The search for storage concepts that can guarantee the safe storage and isolation of radioactive waste is, therefore, another challenging task for materials science, requiring a close examination of natural (geological) materials and processes.

The more than 50 years of research and development of fission and fusion reactors have undoubtedly demonstrated that the statement 'technologies are enabled by materials' is particularly true for nuclear technology. Although the nuclear field is typically known for its incremental progress, the challenges posed by the next generation of fission reactors (Generation IV) as well as the demonstration of fusion reactors will need breakthroughs to achieve their ambitious goals. This is being accompanied by an important change in materials science, with a shift of discovery through experiments to discovery through simulation. The progress in numerical simulation of the material evolution on a scientific and engineering scale is growing rapidly. Simulation techniques at the atomistic or meso scale (e.g., electronic structure calculations, molecular dynamics, kinetic Monte Carlo) are increasingly helping to unravel the complex processes occurring in materials under extreme conditions and to provide an insight into the causes and thus helping to design remedies.

In this context, *Comprehensive Nuclear Materials* aims to provide fundamental information on the vast variety of materials employed in the broad field of nuclear technology. But to do justice to the comprehensiveness of the work, fundamental issues are also addressed in detail, as well as the basics of the emerging numerical simulation techniques.

R.J.M. Konings
European Commission, Joint Research Centre,
Institute for Transuranium Elements, Karlsruhe, Germany

T.R. Allen
Department of Engineering Physics,
Wisconsin University, Madison, WI, USA

R. Stoller
Materials Science and Technology Division,
Oak Ridge National Laboratory, Oak Ridge, TN, USA

S. Yamanaka
Division of Sustainable Energy and Environmental Engineering,
Graduate School of Engineering, Osaka University, Osaka, Japan

FOREWORD

'Nuclear materials' denotes a field of great breadth and depth, whose topics address applications and facilities that depend upon nuclear reactions. The major topics within the field are devoted to the materials science and engineering surrounding fission and fusion reactions in energy conversion reactors. Most of the rest of the field is formed of the closely related materials science needed for the effects of energetic particles on the targets and other radiation areas of charged particle accelerators and plasma devices. A more complete but also more cumbersome descriptor thus would be 'the science and engineering of materials for fission reactors, fusion reactors, and closely related topics.' In these areas, the very existence of such technologies turns upon our capabilities to understand the physical behavior of materials. Performance of facilities and components to the demanding limits required is dictated by the capabilities of materials to withstand unique and aggressive environments. The unifying concept that runs through all aspects is the effect of radiation on materials. In this way, the main feature is somewhat analogous to the unifying concept of elevated temperature in that part of materials science and engineering termed 'high-temperature materials.'

Nuclear materials came into existence in the 1950s and began to grow as an internationally recognized field of endeavor late in that decade. The beginning in this field has been attributed to presentations and discussions that occurred at the First and Second International Conferences on the Peaceful Uses of Atomic Energy, held in Geneva in 1955 and 1958. *Journal of Nuclear Materials*, which is the home journal for this area of materials science, was founded in 1959. The development of nuclear materials science and engineering took place in the same rapid growth time period as the parent field of materials science and engineering. And similarly to the parent field, nuclear materials draws together the formerly separate disciplines of metallurgy, solid-state physics, ceramics, and materials chemistry that were early devoted to nuclear applications. The small priesthood of first researchers in half a dozen countries has now grown to a cohort of thousands, whose home institutions are anchored in more than 40 nations.

The prodigious work, '*Comprehensive Nuclear Materials*,' captures the essence and the extensive scope of the field. It provides authoritative chapters that review the full range of endeavor. In the present day of glance and click 'reading' of short snippets from the internet, this is an old-fashioned book in the best sense of the word, which will be available in both electronic and printed form. All of the main segments of the field are covered, as well as most of the specialized areas and subtopics. With well over 100 chapters, the reader finds thorough coverage on topics ranging from fundamentals of atom movements after displacement by energetic particles to testing and engineering analysis methods of large components. All the materials classes that have main application in nuclear technologies are visited, and the most important of them are covered in exhaustive fashion. Authors of the chapters are practitioners who are at the highest level of achievement and knowledge in their respective areas. Many of these authors not only have lived through a substantial part of the history sketched above, but they themselves are the architects. Without those represented here in the author list, the field would certainly be a weaker reflection of itself. It is no small feat that so many of my distinguished colleagues could have been persuaded to join this collective endeavor and to make the real sacrifices entailed in such time-consuming work. I congratulate the Editor, Rudy Konings, and

the Associate Editors, Roger Stoller, Todd Allen, and Shinsuke Yamanaka. This book will be an important asset to young researchers entering the field as well as a valuable resource to workers engaged in the enterprise at present.

Dr. Louis K. Mansur
Oak Ridge, Tennessee, USA

Permission Acknowledgments

The following material is reproduced with kind permission of Cambridge University Press

Figure 15 of Oxide Dispersion Strengthened Steels
Figure 15 of Minerals and Natural Analogues
Table 10 of Spent Fuel as Waste Material
Figure 21b of Radiation-Induced Effects on Microstructure
www.cambridge.org

The following material is reproduced with kind permission of American Chemical Society

Figure 2 of Molten Salt Reactor Fuel and Coolant
Figure 22 of Molten Salt Reactor Fuel and Coolant
Table 9 of Molten Salt Reactor Fuel and Coolant
Figure 6 of Thermodynamic and Thermophysical Properties of the Actinide Nitrides
www.acs.org

The following material is reproduced with kind permission of Wiley

Table 3 of Properties and Characteristics of SiC and SiC/SiC Composites
Table 4 of Properties and Characteristics of SiC and SiC/SiC Composites
Table 5 of Properties and Characteristics of SiC and SiC/SiC Composites
Figure 5 of Advanced Concepts in TRISO Fuel
Figure 6 of Advanced Concepts in TRISO Fuel
Figure 30 of Material Performance in Supercritical Water
Figure 32 of Material Performance in Supercritical Water
Figure 19 of Tritium Barriers and Tritium Diffusion in Fusion Reactors
Figure 9 of Waste Containers
Figure 13 of Waste Containers
Figure 21 of Waste Containers
Figure 11 of Carbide Fuel
Figure 12 of Carbide Fuel
Figure 13 of Carbide Fuel
Figure 4 of Thermodynamic and Thermophysical Properties of the Actinide Nitrides
Figure 2 of The U–F system
Figure 18 of Fundamental Point Defect Properties in Ceramics
Table 1 of Fundamental Point Defect Properties in Ceramics
Figure 17 of Radiation Effects in SiC and SiC-SiC
Figure 21 of Radiation Effects in SiC and SiC-SiC
Figure 6 of Radiation Damage in Austenitic Steels
Figure 7 of Radiation Damage in Austenitic Steels
Figure 17 of Ceramic Breeder Materials
Figure 33a of Carbon as a Fusion Plasma-Facing Material
Figure 34 of Carbon as a Fusion Plasma-Facing Material

Figure 39 of Carbon as a Fusion Plasma-Facing Material
Figure 40 of Carbon as a Fusion Plasma-Facing Material
Table 5 of Carbon as a Fusion Plasma-Facing Material
www.wiley.com

The following material is reproduced with kind permission of Springer

Figure 4 of Neutron Reflector Materials (Be, Hydrides)
Figure 6 of Neutron Reflector Materials (Be, Hydrides)
Figure 1 of Properties and Characteristics of SiC and SiC/SiC Composites
Figure 3 of Properties and Characteristics of SiC and SiC/SiC Composites
Figure 4 of Properties and Characteristics of SiC and SiC/SiC Composites
Figure 5 of Properties and Characteristics of SiC and SiC/SiC Composites
Figure 6 of Properties and Characteristics of SiC and SiC/SiC Composites
Figure 7 of Properties and Characteristics of SiC and SiC/SiC Composites
Figure 8 of Properties and Characteristics of SiC and SiC/SiC Composites
Figure 9 of Properties and Characteristics of SiC and SiC/SiC Composites
Figure 10 of Properties and Characteristics of SiC and SiC/SiC Composites
Figure 11 of Properties and Characteristics of SiC and SiC/SiC Composites
Figure 12 of Properties and Characteristics of SiC and SiC/SiC Composites
Figure 22d of Fission Product Chemistry in Oxide Fuels
Figure 3 of Behavior of LWR Fuel During Loss-of-Coolant Accidents
Figure 14a of Irradiation Assisted Stress Corrosion Cracking
Figure 14b of Irradiation Assisted Stress Corrosion Cracking
Figure 14c of Irradiation Assisted Stress Corrosion Cracking
Figure 25a of Irradiation Assisted Stress Corrosion Cracking
Figure 25b of Irradiation Assisted Stress Corrosion Cracking
Figure 1 of Properties of Liquid Metal Coolants
Figure 5b of Fast Spectrum Control Rod Materials
Figure 3 of Oxide Fuel Performance Modeling and Simulations
Figure 8 of Oxide Fuel Performance Modeling and Simulations
Figure 10 of Oxide Fuel Performance Modeling and Simulations
Figure 11 of Oxide Fuel Performance Modeling and Simulations
Figure 14 of Oxide Fuel Performance Modeling and Simulations
Figure 5 of Thermodynamic and Thermophysical Properties of the Actinide Nitrides
Figure 51 of Phase Diagrams of Actinide Alloys
Figure 6 of Thermodynamic and Thermophysical Properties of the Actinide Oxides
Figure 7b of Thermodynamic and Thermophysical Properties of the Actinide Oxides
Figure 9b of Thermodynamic and Thermophysical Properties of the Actinide Oxides
Figure 35 of Thermodynamic and Thermophysical Properties of the Actinide Oxides
Table 11 of Thermodynamic and Thermophysical Properties of the Actinide Oxides
Table 13 of Thermodynamic and Thermophysical Properties of the Actinide Oxides
Table 17 of Thermodynamic and Thermophysical Properties of the Actinide Oxides
Figure 18 of Radiation Damage of Reactor Pressure Vessel Steels
Figure 7 of Radiation Damage Using Ion Beams
Figure 9b of Radiation Damage Using Ion Beams
Figure 28 of Radiation Damage Using Ion Beams
Figure 34 of Radiation Damage Using Ion Beams
Figure 35 of Radiation Damage Using Ion Beams
Figure 36d of Radiation Damage Using Ion Beams
Figure 37 of Radiation Damage Using Ion Beams
Table 3 of Radiation Damage Using Ion Beams

Figure 5 of Radiation Effects in UO_2
Figure 9a of *Ab Initio* Electronic Structure Calculations for Nuclear Materials
Figure 9b of *Ab Initio* Electronic Structure Calculations for Nuclear Materials
Figure 9c of *Ab Initio* Electronic Structure Calculations for Nuclear Materials
Figure 10a of *Ab Initio* Electronic Structure Calculations for Nuclear Materials
Figure 23 of Thermodynamic and Thermophysical Properties of the Actinide Carbides
Figure 25 of Thermodynamic and Thermophysical Properties of the Actinide Carbides
Figure 26 of Thermodynamic and Thermophysical Properties of the Actinide Carbides
Figure 27 of Thermodynamic and Thermophysical Properties of the Actinide Carbides
Figure 28a of Thermodynamic and Thermophysical Properties of the Actinide Carbides
Figure 28b of Thermodynamic and Thermophysical Properties of the Actinide Carbides
Figure 2 of Physical and Mechanical Properties of Copper and Copper Alloys
Figure 5 of Physical and Mechanical Properties of Copper and Copper Alloys
Figure 6 of The Actinides Elements: Properties and Characteristics
Figure 10 of The Actinides Elements: Properties and Characteristics
Figure 11 of The Actinides Elements: Properties and Characteristics
Figure 12 of The Actinides Elements: Properties and Characteristics
Figure 15 of The Actinides Elements: Properties and Characteristics
Table 1 of The Actinides Elements: Properties and Characteristics
Table 6 of The Actinides Elements: Properties and Characteristics
Figure 25 of Fundamental Properties of Defects in Metals
Table 1 of Fundamental Properties of Defects in Metals
Table 7 of Fundamental Properties of Defects in Metals
Table 8 of Fundamental Properties of Defects in Metals
www.springer.com

The following material is reproduced with kind permission of Taylor & Francis

Figure 9 of Radiation-Induced Segregation
Figure 6 of Radiation Effects in Zirconium Alloys
Figure 1 of Dislocation Dynamics
Figure 25 of Radiation Damage Using Ion Beams
Figure 26 of Radiation Damage Using Ion Beams
Figure 27 of Radiation Damage Using Ion Beams
Figure 4 of Radiation-Induced Effects on Material Properties of Ceramics (Mechanical and Dimensional)
Figure 7 of The Actinides Elements: Properties and Characteristics
Figure 20 of The Actinides Elements: Properties and Characteristics
Figure 18a of Primary Radiation Damage Formation
Figure 18b of Primary Radiation Damage Formation
Figure 18c of Primary Radiation Damage Formation
Figure 18d of Primary Radiation Damage Formation
Figure 18e of Primary Radiation Damage Formation
Figure 18f of Primary Radiation Damage Formation
Figure 1 of Radiation-Induced Effects on Microstructure
Figure 27 of Radiation-Induced Effects on Microstructure
Figure 5 of Performance of Aluminum in Research Reactors
Figure 2 of Atomic-Level Dislocation Dynamics in Irradiated Metals
Figure 3 of Atomic-Level Dislocation Dynamics in Irradiated Metals
Figure 5 of Atomic-Level Dislocation Dynamics in Irradiated Metals
Figure 10a of Atomic-Level Dislocation Dynamics in Irradiated Metals
Figure 10b of Atomic-Level Dislocation Dynamics in Irradiated Metals
Figure 10c of Atomic-Level Dislocation Dynamics in Irradiated Metals

Figure 10d of Atomic-Level Dislocation Dynamics in Irradiated Metals
Figure 12a of Atomic-Level Dislocation Dynamics in Irradiated Metals
Figure 12b of Atomic-Level Dislocation Dynamics in Irradiated Metals
Figure 12c of Atomic-Level Dislocation Dynamics in Irradiated Metals
Figure 12d of Atomic-Level Dislocation Dynamics in Irradiated Metals
Figure 16a of Atomic-Level Dislocation Dynamics in Irradiated Metals
Figure 16b of Atomic-Level Dislocation Dynamics in Irradiated Metals
Figure 16c of Atomic-Level Dislocation Dynamics in Irradiated Metals
Figure 16d of Atomic-Level Dislocation Dynamics in Irradiated Metals
Figure 16e of Atomic-Level Dislocation Dynamics in Irradiated Metals
Figure 17a of Atomic-Level Dislocation Dynamics in Irradiated Metals
Figure 17b of Atomic-Level Dislocation Dynamics in Irradiated Metals
Figure 17c of Atomic-Level Dislocation Dynamics in Irradiated Metals
Figure 17d of Atomic-Level Dislocation Dynamics in Irradiated Metals
www.taylorandfrancisgroup.com

4.01 Radiation Effects in Zirconium Alloys

F. Onimus and J. L. Béchade
Commissariat à l'Energie Atomique, Gif-sur-Yvette, France

4.01.1	**Irradiation Damage in Zirconium Alloys**	2
4.01.1.1	Damage Creation: Short-Term Evolution	2
4.01.1.1.1	Neutron–zirconium interaction	2
4.01.1.1.2	Displacement energy in zirconium	2
4.01.1.1.3	Displacement cascade in zirconium	2
4.01.1.2	Evolution of Point Defects in Zirconium: Long-Term Evolution	4
4.01.1.2.1	Vacancy formation and migration energies	4
4.01.1.2.2	SIA formation and migration energies	4
4.01.1.2.3	Evolution of point defects: Impact of the anisotropic diffusion of SIAs	6
4.01.1.3	Point-Defect Clusters in Zirconium Alloys	7
4.01.1.3.1	⟨*a*⟩ Dislocation loops	7
4.01.1.3.2	⟨*a*⟩ Loop formation: Mechanisms	8
4.01.1.3.3	⟨*c*⟩ Component dislocation loops	9
4.01.1.3.4	⟨*c*⟩ Loop formation: Mechanisms	9
4.01.1.3.5	Void formation	10
4.01.1.4	Secondary-Phase Evolution Under Irradiation	10
4.01.1.4.1	Crystalline to amorphous transformation of Zr-(Fe,Cr,Ni) intermetallic precipitates	10
4.01.1.4.2	Irradiation effects in Zr–Nb alloys: Enhanced precipitation	13
4.01.2	**Postirradiation Mechanical Behavior**	14
4.01.2.1	Mechanical Behavior During Tensile Testing	14
4.01.2.1.1	Irradiation hardening: Macroscopic behavior	14
4.01.2.1.2	Irradiation hardening: Mechanisms	14
4.01.2.1.3	Post-yield deformation: Macroscopic behavior	16
4.01.2.1.4	Post-yield deformation: Mechanisms	16
4.01.2.2	Effect of Postirradiation Heat Treatment	17
4.01.2.3	Postirradiation Creep	18
4.01.3	**Deformation Under Irradiation**	19
4.01.3.1	Irradiation Growth	19
4.01.3.1.1	Irradiation growth: Macroscopic behavior	19
4.01.3.1.2	Irradiation growth: Mechanisms	21
4.01.3.2	Irradiation Creep	24
4.01.3.2.1	Irradiation creep: Macroscopic behavior	24
4.01.3.2.2	Irradiation creep: Mechanisms	25
4.01.3.3	**Outlook**	26
References		27

Abbreviations

BWR	Boiling-water reactor
CANDU	Canadian deuterium uranium
DAD	Diffusion anisotropy difference
EAM	Embedded atom method
EID	Elastic interaction difference
FP-LMTO	Full-potential linear muffin-tin orbital
GGA	Generalized gradient approximation
hcp	Hexagonal close-packed
HVEM	High-voltage electron microscope
LDA	Local density approximation
MB	Many body
MD	Molecular dynamics
NRT	Norgett–Robinson–Torrens

PKA	Primary knocked-on atom
PWR	Pressurized water reactor
RXA	Recrystallization annealed
SANS	Small-angle neutron scattering
SIA	Self interstitial atom
SIPA	Stress-induced preferential absorption
SIPA-AD	Stress preferential induced nucleation-anisotropic diffusion
SIPN	Stress preferential induced nucleation
SRA	Stress-relieved annealed
TEM	Transmission electron microscopy
Tm	Melting temperature
UTS	Ultimate tensile strength
YS	Yield stress

4.01.1 Irradiation Damage in Zirconium Alloys

4.01.1.1 Damage Creation: Short-Term Evolution

4.01.1.1.1 Neutron–zirconium interaction

Zirconium alloys are used as structural components for light and heavy water nuclear reactor cores because of their low capture cross section to thermal neutrons and their good corrosion resistance. In a nuclear reactor core, zirconium alloys are subjected to a fast neutron flux ($E > 1$ MeV), which leads to irradiation damage of the material. In the case of metallic alloys, the irradiation damage is mainly due to elastic interaction between fast neutrons and atoms of the alloy that displace atoms from their crystallographic sites (depending on the energy of the incoming neutron) and can create point defects without modifications of the target atom, as opposed to inelastic interactions leading to transmutation, for instance. During the collision between the neutron and the atom, part of the kinetic energy can be transferred to the target atom. The interaction probability is given by the elastic collision differential cross section[1,2] which depends on both the neutron kinetic energy and the transferred energy.[3] For a typical fast neutron of 1 MeV, the mean transferred energy ($\bar{T}$) of the Zr atom is $\bar{T} \approx 22$keV. For low value of the transferred energy, the target atom cannot leave its position in the crystal, leading only to an increase of the atomic vibrational amplitude resulting in simple heating of the crystal. If the transferred energy is higher than a threshold value, the displacement energy (E_d), the knocked-on atom can escape from its lattice site and is called the primary knocked-on atom (PKA). For high transferred energy, as is the case for fast neutron irradiation, the PKA interacts with the other atoms of the alloy along its track. On average, at each atomic collision, half of its current kinetic energy is transferred to the collided atom, since they have equal masses. The collided atoms can then interact with other atoms, thus creating a displacement cascade within the crystal.

4.01.1.1.2 Displacement energy in zirconium

In the case of zirconium, the displacement energy has been measured experimentally using electron irradiations performed at low temperatures (<10 K). The irradiation damage was monitored *in situ* using electrical resistivity changes.[4,5] The measured minimum displacement threshold energy transferred to the Zr atoms is $E_d = 21$–24 eV. Measurements of E_d have also been performed using a high-voltage electron microscope (HVEM) to irradiate a Zr thin foil. The values obtained were found to be weakly orientation dependent, between 24 and 27.5 eV, with a mean $\bar{E}_d$ of 24 eV.[6]

The displacement energy has also been computed by molecular dynamics (MD) simulations based on various interatomic potentials. The most accurate computations have been performed using a many-body (MB) potential based on the Finnis and Sinclair formalism.[7] These authors have found that the displacement energy is significantly anisotropic. Displacement energy was found to be minimum for knocking out in the basal plane, that is, in the $\langle 11\bar{2}0 \rangle$ directions, corresponding to the most favorable direction for replacement collision sequences, and to the direction of development of the basal crowdion. The corresponding displacement energy obtained ($E_d = 27.5$ eV) is slightly above the experimental values. The value averaged over all the crystallographic directions was found to be 55 eV. The value specified in the norm reference test standard (Standard E521–89, Annual Book of ASTM Standards, ASTM, Philadelphia, PA, USA) is $\bar{E}_d = 40$ eV.[8] This value is close to the spatial means obtained by MD models.

4.01.1.1.3 Displacement cascade in zirconium

The number of displaced atoms inside the cascade can be simply estimated using the Kichin–Pease formula[9] or the modified Kichin–Pease formula (Norgett–Robinson–Torrens model or NRT model).[10,11] According to this last model, the number of displaced atoms within the cascade in the case of a 22 keV PKA and using a displacement energy of $E_d = 40$ eV is $n_p = 0.4\bar{E}_T/E_d \approx 220$. Because of the large mean free path of fast neutrons (several

centimeters), it can be considered that only one PKA is created by the incoming neutron going through the Zr cladding used in pressurized water reactors (PWRs) (with a thickness of 0.6 mm). Therefore, if the PKA creation rate per unit volume within the cladding is known for a typical fuel assembly in a PWR (with typical fast neutron flux is 5×10^{17} n m^{-2} s^{-1} ($E > 1$ MeV)), the number of displaced atoms per unit volume and per second can be computed. From this value, the overall number of displacements per atom (dpa) and per second can be simply computed. This calculation can be achieved, as described by Lunéville *et al.*,[3] by taking into account the PWR neutron spectrum as well as the neutron–atom differential cross section. It can be shown that a typical damage rate for a cladding in a PWR core is between 2 and 5 dpa year^{-1}, depending on the neutron flux history. This means that each atom of the cladding has been displaced 2–5 times per year! A more accurate correspondence between the fast fluence and the damage for a cladding in a PWR is provided by Shishov *et al.*[12] These authors evaluate that a fluence of 6×10^{24} n m^{-2} ($E > 1$ MeV) corresponds to a damage of 1 dpa.

This simple approach gives a good description of the number of displaced atoms during the creation of the cascade, but does not consider intracascade elastic recombinations that occur during the cascade relaxation or cooling-down phase.[11,13,14] In addition, this approach does not give any information on the form of the remaining damage at the end of the cascade, such as the point-defect clusters that can be created in the cascade.

In order to have a better understanding of the created damage in α-zirconium, several authors have performed MD computations also using different types of interatomic potentials. It is shown that, at the end of the cascade creation (<2 ps), the cascade is composed of a core with a high vacancy concentration, and the self interstitial atoms (SIAs) are concentrated at the cascade periphery.[14–16] The cascade creation is followed by the athermal cascade relaxation that can last for a few picoseconds. During this phase, most of the displaced atoms quickly reoccupy lattice sites as a result of prompt (less than a lattice vibration period, 0.1 ps) elastic recombination if a SIA and a vacancy are present at the same time in the elastic recombination volume (with 200 $\Omega < V_r < 400$ Ω, where V_r is the elastic recombination volume and Ω the atomic volume.[17]) Wooding *et al.*[16] and Gao *et al.*[8] have shown that at the end of the cascade relaxation the number of surviving point defects is very low, much lower, only 20% at 600 K, than the number of Frenkel pairs computed using the NRT model. It is also shown that all the point defects are not free to migrate but that small point-defect clusters are created within the cascade. This clustering is due to short-range diffusion driven by the large elastic interaction among neighboring point defects and small point-defect clusters. In the case of zirconium, large point-defect clusters, up to 24 vacancies and 25 SIAs (at 600 K), can be found at the end of the cascade relaxation (**Figure 1**).[8] According to Woo *et al.*,[14] the presence of these small point-defect clusters spatially separated from each other, as well as the different concentrations of single vacancies and SIAs, can have a major impact on the subsequent microstructural evolution. This effect is known as the production bias, which has to be considered when solving the rate equations in the mean-field approach of point-defect evolution.[14]

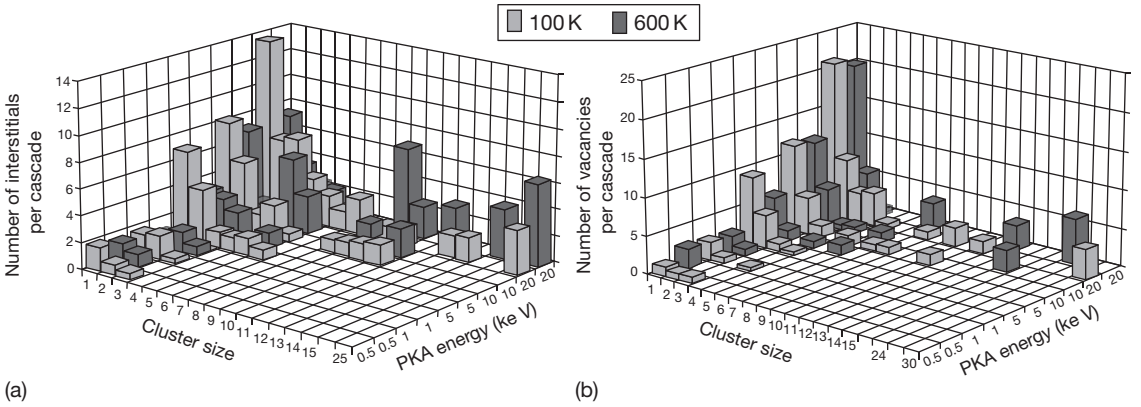

Figure 1 Number of single and clustered (a) interstitials and (b) vacancies per cascade as a function of the PKA energy. Adapted from Gao, F.; Bacon, D. J.; Howe, L. M.; So, C. B. *J. Nucl. Mater.* **2001**, *294*, 288–298.

The form of these small clusters is also of major importance since it plays a role on the nucleation of dislocation loops. Wooding *et al.*[16] and Gao *et al.*[8] have shown that the small SIA clusters are in the form of dislocation loops with the Burgers vector $1/3\langle 11\bar{2}0\rangle$. The collapse of the 24-vacancy cluster to a dislocation loop on the prism plane was also found to occur.

4.01.1.2 Evolution of Point Defects in Zirconium: Long-Term Evolution

After the cascade formation and relaxation, which last for a few picoseconds, the microstructure evolves over a longer time. The evolution of the microstructure is driven by the bulk diffusion of point defects. For a better understanding of the microstructure evolution under irradiation, the elementary properties of point defects, such as formation energy and migration energy, have first to be examined.

4.01.1.2.1 Vacancy formation and migration energies

Concerning the vacancy, all the atomic positions are identical in the lattice and so there is only one vacancy description leading to a unique value for the vacancy formation energy. Due to the rather low α–β phase transformation temperature, the measurement of vacancy formation and migration energy in the Zr hexagonal close-packed (hcp) phase is difficult. The temperature that can be reached is not high enough to obtain an accurately measurable concentration and mobility of vacancies.[18] Nevertheless, various experimental techniques (**Table 1**), such as positron annihilation spectroscopy or diffusion of radioactive isotopes, have been used in order to measure the vacancy formation and migration energies or the self-diffusion coefficient.[18–26] The values obtained by the various authors are given in **Table 1**. It is pointed out by Hood[18] that there is great discrepancy among the various results. It is particularly shown that at high temperature, the self-diffusion activation energy is rather low compared to the usual self-diffusion activation energy in other metals.[18] However, as the temperature decreases, the self-diffusion activation energy increases strongly. According to Hood,[18] this phenomenon can be explained assuming that at high temperature the vacancy mobility is enhanced by some impurity such as an ultrafast species like iron. At lower temperature, the iron atoms are believed to form small precipitates, explaining that at low temperatures the measured self-diffusion energy is coherent with usual intrinsic self-diffusion of hcp crystals. It is also shown that the self-diffusion anisotropy remains low for normal-purity zirconium, with a slightly higher mobility in the basal plane than along the $\langle c\rangle$ axis.[22,26,27] For high-purity zirconium, with a very low iron content, the anisotropy is reversed, with a higher mobility along the $\langle c\rangle$ axis than in the basal plane.[27]

Table 1 Experimental determination formation (E_f), migration (E_m) and self diffusion activation (E_a) energies for vacancy (in eV)

Experimental methods	E_f	E_m	E_a	*Reference*
Semiempirical	1.8–1.9	1.3–1.6	3.3	[18]
Self-diffusion	–	–	1.2–3.5	[18]
Diffusion behavior of various solutes in Zr	1.4–2.1	1.1–1.5	3.2–3.5	[19]
Self-diffusion	–	–	2.85	[20]

The vacancy formation and migration energies have also been computed either by MD methods, where the mean displacement distance versus time allows obtaining the diffusion coefficient, or by static computation of the energy barrier corresponding to the transition between two positions of the vacancy using either empirical interatomic potential[7,28–34] or the most recent *ab initio* tools.[35–38] Since the different sites surrounding the vacancy are not similar, due to the non-ideal c/a ratio, the migration energies are expected to depend on the crystallographic direction, that is, the migration energies in the basal plane $E_m^{//}$ and along the $\langle c\rangle$ direction $E_m^{\perp}$ are different. The results are given in **Table 2.**

The atomistic calculations are in agreement with the positron annihilation spectroscopy measurement but are in disagreement with the direct measurements of self-diffusion in hcp zirconium.[20] As discussed by Hood,[18] and recently modeled by several authors,[39,40] this phenomenon is attributed to the enhanced diffusion due to coupling with the ultrafast diffusion of iron.

4.01.1.2.2 SIA formation and migration energies

In the case of SIAs, the insertion of an additional atom in the crystal lattice leads to a great distortion of the lattice. Therefore, only a limited number of configurations are possible. The geometrical description of all the interstitial configuration sites has been